Desalination and Water Treatment
www.deswater.com

doi: 10.5004/dwt.2020.26287

204 (2020) 50–58
November

Evaluation of the operation seawater and brackish water desalination system using two-pass nanofiltration

Catalina Vargas, Rodrigo Bórquez*

Chemical Engineering Department, Universidad de Concepción, Chile, emails: rborquez@udec.cl (R. Bórquez), catavargas@udec.cl (C. Vargas)

Received 31 January 2020; Accepted 21 June 2020

ABSTRACT

The lack of freshwater supply in the rural coastal village in Chile has motivated the implementation of a pilot-size nanofiltration desalination plant. The objective of this study was to evaluate the seawater and brackish water desalination system using two-pass nanofiltration. The system achieved a permeate recovery of 21.0 L/(m^2 h) and 51.3 L/(m^2 h) in the first pass at 40 bar and in the second pass at 15 bar, respectively. As the quality of water obtained in the first pass was satisfactory, it was mixed with water from the second pass, resulting in safe drinking water that conforms to local and international standards. At present, this system supplies drinking water to a coastal village of Chile and can be used to treat different types of brackish water and be coupled with renewable energies. It can provide potable water at a cost of US $ 0.70/m^3, which is a competitive price considering the small size of the system.

Keywords: Desalination; Nanofiltration; Pilot plant; Drinking water

1. Introduction

Lack of water resources for consumption and industrial use is one of the greatest concerns worldwide. According to the United Nations Educational, Scientific, and Cultural Organization (UNESCO), it has been estimated that two-thirds of the world's population will be living under water stress by 2025 [1]. Chile has some of the driest areas in the world, and the human activities in these areas require large volumes of water, resulting in high water scarcity that has led to environmental degradation, conflicts and reduced industrial productivity [2]. For instance, desalination is playing a fundamental role to face the problem of water scarcity in northern Chile, where conventional water resources are very limited or even non-existent [3].

Methods such as seawater desalination can be used to solve this problem. Desalinated water production has grown rapidly in the past decade, especially in arid coastal zones. The total installed capacity increased by 57% annually between 2008 and 2013, achieving a production level of 80 million m^3/d of water in 2013. According to the International Desalination Association (IDA), there were around 16,000 desalination plants in operation in 150 countries by 2015, producing 90 million m^3/d of desalinated water [4,5]. Desalination costs have dropped by 50% in recent decades because of the development of new and modified membranes, and the implementation of energy recovery systems. Which makes membrane technology increasingly attractive compared to other alternatives [6].

At present, the desalination industry is dominated by reverse osmosis (RO) [7]. This membrane-based process exceeds the installed capacity of thermal systems (multi-stage flash evaporation and multiple-effect distillation), which are widely used in the Gulf Cooperation Council (GCC) and the Middle East–North Africa (MENA). Great efforts have been made to improve efficiency and reduce energy consumption in desalination processes. However, the implementation of seawater desalination systems continues to be a challenge due to the operating costs associated with high operating pressures and fouling by divalent ions [8].

* Corresponding author.

Nanofiltration (NF) is considered as an effective membrane process [9–11]. The pore sizes of NF lie between those of RO and UF membranes. NF operates at lower transmembrane pressures (TMP), generates greater permeate fluxes, and requires lower investment costs as compared to RO. Additionally, NF has a high removal (high rejection) of divalent ions, especially anions [12]. Due to all these characteristics, NF is gaining importance in seawater desalination [13]. There are some alternatives based on the use of NF for seawater desalination, such as the two-stage nanofiltration process developed by Gouellec [14]. This technique reduces energy consumption by up to 20%–30% as compared to RO [15]. It was reported to be applied at a production scale in Long Beach (USA), obtaining a flow of 1,135 m^3/d of drinking water. TMP of each NF stage significantly affects the generated water flow and total dissolved solids (TDS) of the water within the operational parameters considered in this system [16].

NF is a very complex process that depends on microhydrodynamics and interfacial events that take place on the membrane surface and inside the nanopores. In this process, a combination of steric, Donnan, dielectric, and transport effects causes rejection. The dissociation of ionizable groups on the membrane surface and inside the pores generates the charge in the membrane [17]. The dissociation of these surface groups strongly depends on the pH of the contact solution; the membrane can exhibit an isoelectric point at a given pH when membrane surface chemistry is amphoteric [18]. NF membranes also have a weak ion-exchange capacity. Therefore, some ions can be adsorbed on the membrane surface, thus causing a slight modification in the surface charge [19]. Electrostatic repulsion or attraction occurs according to ion valence and the fixed charge of the membrane.

Membrane fouling is a key factor affecting both the competitiveness and effectiveness of the process in terms of costs. Fouling can cause negative effects, such as flux decrease (productivity loss), increased operating costs due to increased energy demand, increased membrane maintenance, and cleaning, excessive chemical use, and even reduced membrane lifetime. Therefore, effective fouling control and mitigation are crucial to reducing these adverse effects. Removing the largest possible amount of water contaminants associated with the phenomenon before the NF operation is a widely used strategy to prevent fouling. Moreover, microfiltration (MF) is considered as one of the most frequently applied operations, even though there are different pretreatments in NF and RO operations [20].

This study focuses on the implementation and evaluation of a pilot-scale desalination system using two-pass nanofiltration to determine optimal operating conditions for seawater and brackish water desalination. The improved NF process (Chilean Patent N° 52855, 2013–2033) presents an adaptable modular system with operational flexibility. Thus, it can be used for seawater and brackish water and allows to obtain drinking water, or water for a range of industrial and domestic purposes that conforms to local regulations (NCh.409) and guidelines of the World Health Organization (WHO), to supply coastal communities with no access to drinking water. As it is a flexible modular system of low production, applications of membrane technology to renewable energy generation can also be considered.

2. Materials and methods

2.1. Characterization of the seawater and brackish water used in the tests

The coastal area of the Bio Bio Region, Chile, was used to supply seawater for the tests in this study. The characteristics of the seawater and brackish water used in the tests are shown in Table 1.

In Table 1, all analyses were carried out according to standard methods [21] in triplicate.

2.3. Desalination plant

A diagram of the operation using two-pass NF in a series is presented in Fig. 1.

The system has a capacity to process up to 9 m^3/h of seawater or brackish water.

As the system operates continuously, the pretreatment was a microfiltration stage, a stage that involves $FeCl_3$ dosing, and the subsequent removal of precipitates in prefiltering. A prefilter (Clack, model YTP2472–4) filled with commercial "clinoptilolite-zeolite" sand was used for precipitate removal. The MF cut off was 1-μm tubular filters (twin pure, polyethylene).

Vitec 4000 (San Diego, United States) antiscalant (4 ppm) was added continuously to reduce scaling formation after the first pass of nanofiltration at the permeate flow. After passing through the MF, turbidity values were lower than those recommended by the manufacturer of the NF90 membrane (DOW Chemical, Michigan, United States). Therefore, the input water met the quality requirements needed to ensure a safe and stable process.

In the first pass of nanofiltration, two modules were operated in parallel. Each module consisted of three

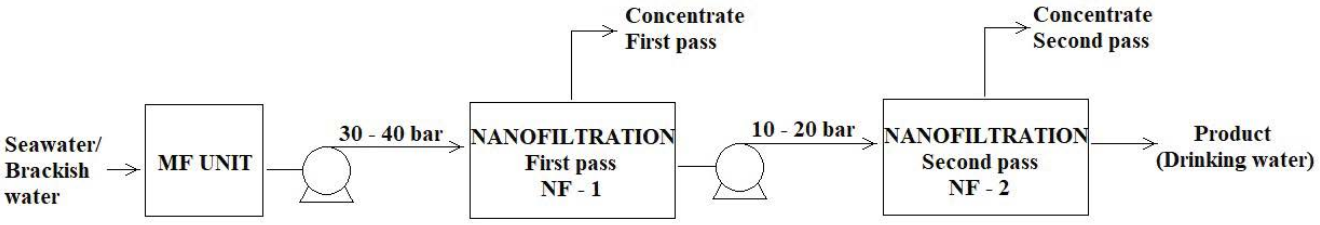

Fig. 1. Scheme of the desalination system using two-pass nanofiltration in series.

membranes, each with a 7.6 m^2 active surface (NF90–4040). The first pass allowed operation at a maximum pressure of 40 bar with recovery between 20% and 25% depending on the feeding condition (salinity and temperature of seawater and brackish water used) and the salinity of rejection for its least impact on the environment. In the second pass of nanofiltration, two modules were operated. Each module consisted of the same type of membranes as in the first pass. The second pass allowed operation at a maximum pressure of 15 bar and was designed to reach a recovery of 70% of permeate from the first pass.

Second-pass NF concentrate was recirculated toward the seawater or brackish water feed because it had low conductivity and turbidity. This recirculation was done to dilute fresh seawater or brackish water and increase salt rejection at the first-pass NF, and also increase recovery and the use of the total water that entered in the second pass. The product water, which conforms to the local standard NCh.409 for drinking water quality, was produced by partially mixing water generated in the first pass with that generated in the second pass.

2.4. Theory equations

The permeate water flux was calculated as:

$$J_w = \frac{\Delta V}{A_m \cdot \Delta t} \tag{1}$$

where $\Delta V/\Delta t$ is the permeate volume over time and A_m is the effective filtration area. The hydraulic permeability constant (k_w) was determined using the following expression:

$$k_w = \frac{J_w}{\Delta P} \tag{2}$$

where ΔP is operational pressure.

Conductivity removal efficiency and ions removal efficiency of seawater were calculated using the expression given below:

$$R = \left(1 - \frac{C_p}{C_f}\right) \times 100 \tag{3}$$

where C_f is the ions conductivity of feed liquid, and C_p is the ions conductivity of permeate liquid.

Finally, water recovery efficiency can be expressed as:

$$Y = \left(\frac{Q_p}{Q_f}\right) \times 100 \tag{4}$$

where Q_p is the amount of permeate (L/h) and Q_f is the quantity of feed (L/h).

3. Results and discussion

3.1. Plant assays with seawater

3.1.1. Determination of the operating pressure in the first pass of NF operating continuously

In order to define the standard of the water produced, optimal operating conditions in the first pass were determined based on the energy consumption under continuous operation. Afterward, the variables that allow the greatest possible product flow at the lowest operational cost in the second pass of nanofiltration were also determined based on the specifications of NCh.409 and the WHO guidelines.

During the six months of continuous operation, characteristics of the seawater were maintained constant. The conductivity and pH values of the seawater used in this study are provided in Table 1.

The variation in the feed pressure for NF-1 was studied during the continuous operation, keeping the rest of the operational variables constant.

As shown in Fig. 2, as the motive power of the feed flow overcomes, the osmotic pressure of the system and the exerted TMP affect the permeate flux [22]. A pressure of up to 40 bar was used as the maximum operating pressure of the NF90 membranes. The diffusion and convection phenomena produced solute transport through a nanofiltration membrane. The process of convection prevailed over diffusion at greater pressures, thus increasing the permeate flux [23].

Electrical conductivity was measured at a 1 h interval in triplicate for the different working pressures. Fig. 2 shows the salt separation obtained in the first pass. It can be observed that the salt conductivity of the permeate decreases with an increase in the pressure of the system [23]. No concentration polarization effects were observed at pressures near 40 bar [22]. At high pressures (36–40 bar), the permeate quality obtained with the membrane was within the expected range, and it was similar to that obtained at lower pressures in biologically treated water [24]. Moreover, high crossflow velocity causes a decrease in electrical conductivity, thus preventing salt from compacting on the rough membrane and allowing better rejection [25].

Table 1
Composition of the seawater and brackish water used in the tests

Parameter	Unit	Seawater	Brackish
pH	–	7.4 ± 0.35	7.4–7.6
Conductivity	μS/cm	51,000 ± 200	29,000–33,000
Hardness	mg $CaCO_3$/L	8,137 ± 20	–
Turbidity	NTU	3.36 ± 1.52	6.46 ± 0.45
Total suspended solids	mg/L	13 ± 1.5	–
TDS	mg/L	32,640	19,800
Chloride	mg/L	19,350 ± 425	11,310
Sulfate	mg/L	2,719 ± 416	1,590
Nitrate	mg/L	<0.023	–
Boron	mg/L	5.48 ± 0.07	–
Sodium	mg/L	11,080 ± 28	7,300
Magnesium	mg/L	1,672 ± 5.4	–
Manganese	mg/L	–	0.20
Calcium	mg/L	502 ± 0.6	–
Iron	mg/L	–	0.8
Potassium	mg/L	516 ± 2.2	–
Ammonium	μg/L	130 ± 14	–
Silicon oxide	mg/L	3.70 ± 2.8	0.038

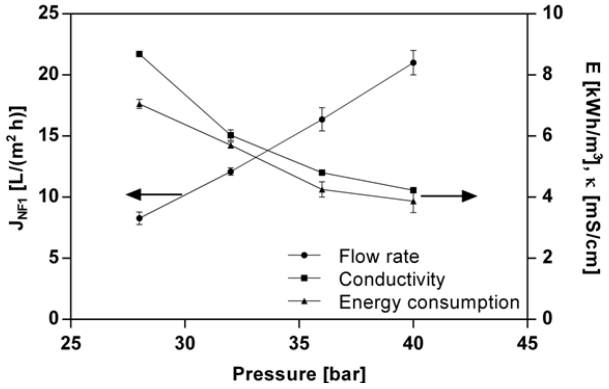

Fig. 2. Effect of pressure on the permeate flux, energy consumption and conductivity in the first pass of seawater nanofiltration. Error bars represent 95% confidence interval of three measurements.

The specific energy consumption (SEC) of the first pass decreased with the applied pressure because the first pass was coupled with an energy recovery device, which uses the rejection energy of this pass to raise the feed pressure increasing the pressure of 67% of the feed flow with 94.7% efficiency according to its manual (PX-30S, ERI). As in RO in nanofiltration energy is recovered and in addition, only a high-pressure pump is required to boost only 33% of the feed water. Liu et al. [16] observed a similar trend in the two-pass nanofiltration in terms of the reduction in the SEC of the process with operational pressure.

Salt rejection in NF-1 was between 91% and 93% for sodium chloride and chloride ions, respectively (Table 2). Despite the high separation, the chemical analysis revealed that water composition did not comply with the Chilean standard NCh.409 and the WHO guidelines for drinking water quality. Therefore, the second pass of nanofiltration was necessary to achieve the required quality of the product. In addition to the low SEC and the greater recovery rate of the NF-1 pass (22.5%), lower product water conductivity is achieved at a pressure of 40 bar (Fig. 2). Recovery was not increased to avoid a high saline rejection and therefore a greater environmental impact in protected areas. As in RO, it is possible in nanofiltration with the same high-pressure pump without higher energy consumption, only increasing the area of membranes reach recoveries between 45% and 50%.

3.1.2. Determination of the operating pressure in the continuously second pass of NF

The increase in the operating pressure resulted in an increase in the flow of produced water while operating independently in the NF-2 pass. Fig. 3 shows that an increase in the pressure in the second pass of nanofiltration produced an increase in the total water produced by the pilot plant during the continuous operation of the system.

The characteristics of the water product obtained in the tests are shown in Table 3. The water product quality complies with the specifications of the Chilean standard NCh.409 and the WHO guidelines.

Table 2
Chemical analysis of the first pass permeates with a recovery of 22.5%

Parameter	Unit	Result
pH	–	6.8 ± 0.2
Conductivity	μS/cm	4,500 ± 19
Hardness	mg $CaCO_3$/L	245 ± 5
Chloride	mg/L	1,350 ± 24
Sulfate	mg/L	5.7 ± 0.7
Nitrate	mg/L	0.4 ± 0.05
Boron	mg/L	1.45 ± 0.15
Sodium	mg/L	2,500 ± 24
Magnesium	mg/L	24 ± 3
Calcium	mg/L	10 ± 1
Potassium	mg/L	125 ± 9
Ammonium	μg/L	0
Carbonate	mg/L	0

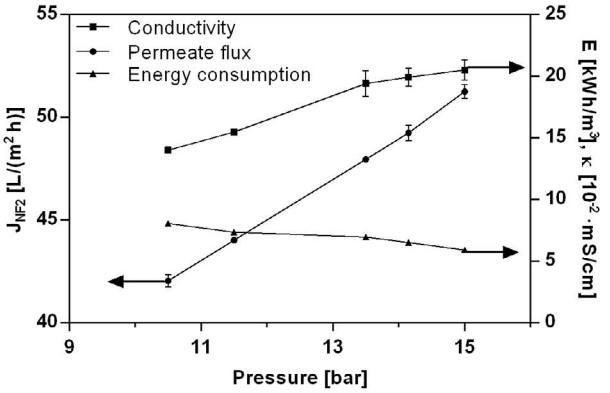

Fig. 3. Effect of pressure on permeate flux, conductivity and total energy consumption in the second pass of seawater nanofiltration (NF-2). Error bars represent 95% confidence interval of three measurements.

Additionally, a significant reduction in boron concentration was observed in the product water (Fig. 4). In fact, seawater naturally contains an average concentration of 4.6 mg/L for this metalloid [26]. At a global level, various standards specify a maximum limit for boron though this parameter is not regulated by the Chilean standard NCh.409. For example, a limit of 1 mg/L is established by the EU [27]. The average boron concentration achieved by the pilot plant is below this limit. High boron concentrations have been observed in drinking water samples and urine samples of people in northern Chile [28].

3.2. Plant assays with brackish water

3.2.1. Plant performance without recycling stream of rejection

The characterization of brackish water indicates low iron content and a lower salinity range than that of seawater (Table 1).

Table 3
Total monovalent salt rejection in the two-pass nanofiltration process

Sample	TDS	Cl^-	NaCl	pH
	(mg/L)	(mg/L)	(mg/L)	
Feed	35,240 ± 104	19,350 ± 287	28,150 ± 63	7.4 ± 0.3
Permeate 1: 40 bar	2,230 ± 27	1,350 ± 24	2,150 ± 15	6.8 ± 0.2
Permeate 2: 15 bar (product water)	122 ± 9	72 ± 5	119 ± 11	6.9 ± 0.2
NCh.409 standard	<1,500	<400	–	6.5–8.5
WHO standard	<1,000	<250	–	6.5–8.5
% First pass rejection	93.65	93.02	91.04	–
% Total rejection	99.65	99.63	99.50	–

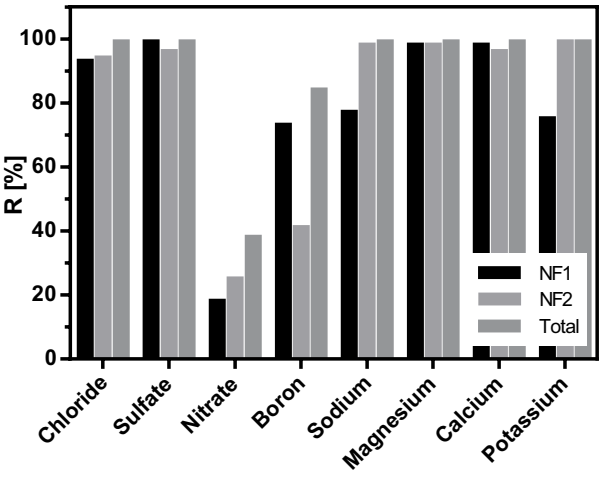

Fig. 4. Total salt rejection in the two-pass nanofiltration process.

As in the case of seawater, in the first pass of nanofiltration, the feeding pressure was varied while maintaining the other constant conditions and the effect on the operation was observed.

In Fig. 5, as in the case of seawater, permeate flux increases linearly with increased pressure, without observing that the critical pressure has been reached [29]. Therefore, like the case of seawater, it was selected as an operating pressure 40–41 bar in the first pass of nanofiltration, where the conductivity of 3.27 mS/cm is obtained.

As shown in Fig. 6, as time passes the water recovery was diminishing. The first days the recovery rate reached 30% until reaching the last days at 13%. On the other hand, the resistance to the transfer of matter shows a constant increase during the 100 d of operation.

The values of conductivity of the water permeate of the NF-1 were practically constant in the time. Although the membrane presented clogging, it still was able to remove high amounts of salts and of the slits that were not retained by the pre-treatments, thus, maintaining a high quality of the water

The SEC of NF pass 1 increased, due to the reduction of the permeate flux. In the beginning, it was 6.9 kWh/m^3 (day 7) and ended with 9.09 kWh/m^3 (day 31).

The average permeate flow was 1.24 m^3/h (27.2 L/m^{2}h), thus, the energy consumption per cubic meter of water was

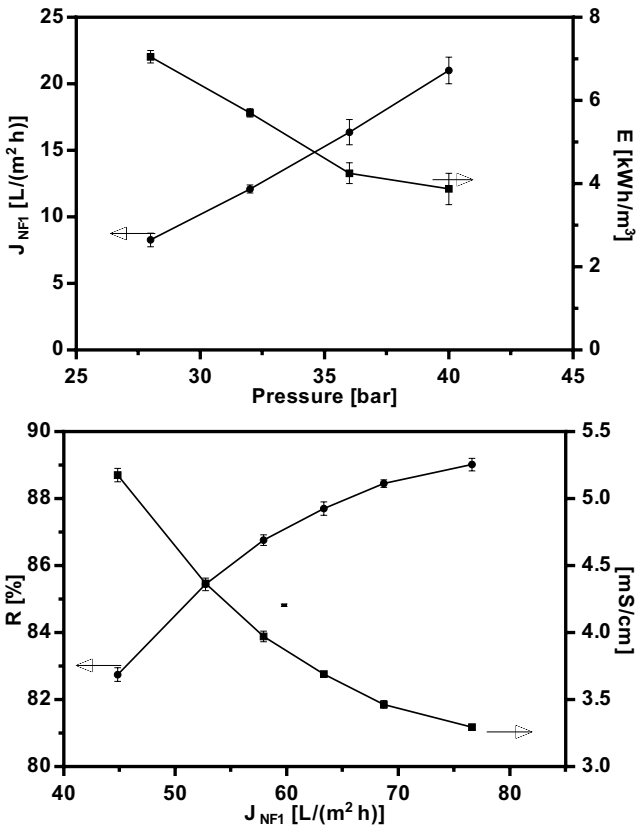

Fig. 5. (a) Effect of pressure on the permeate flux and energy consumption (*E*) and (b) effect of permeate flux on the conductivity and ions rejection in the first pass of brackish water nanofiltration. Error bars represent 95% confidence interval of three measurements.

9.84 kWh/m^3, a consumption greater than that recorded of 9.28 kWh/m^3 using seawater, explained mainly by the presence of colloidal material in the supply water, which affected over time the permeability of the membrane (Table 1, turbidity).

3.2.2. Plant performance with recycling stream of rejection

Pretreatment was modified including two 5 μm microfilters, in addition, the water storage capacity of the first

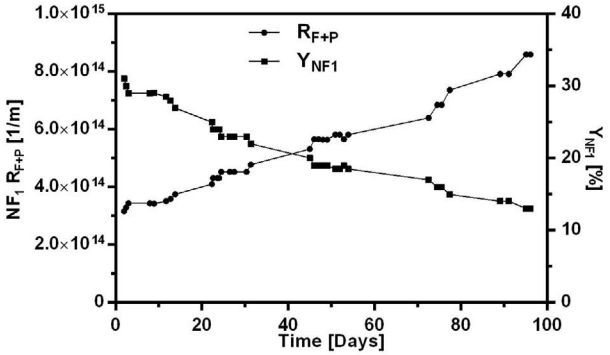

Fig. 6. Mass transfer resistance (fouling) and water recovery during 100 d of continuous operation.

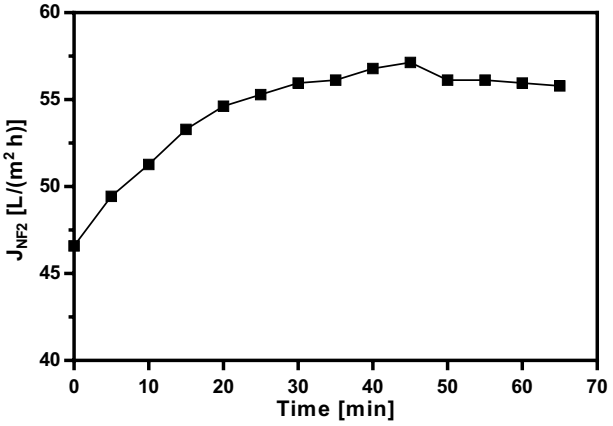

Fig. 7. Variation of permeate flux against time during pass NF-2.

pass of nanofiltration was increased to double and the rejection current was recycled. All these changes were reflected in the autonomy of the plant and greater water production. The permeate flow showed the same linearity ratio in relation to the increase in pressure than the case of the operation without the recycling of rejection.

After one month operating with recycling, the energy consumption was maintained constant (approximately 12.7 kWh/m^3), with the respective elevation compared to the curve obtained from the operation without recycle, due to the lower permeate flow produced with the same energy consumption (Fig. 7). It can be deduced that the effect of the recycle also did not mean a change in the permeate flow of pass NF-1, at least in the time that remained in operation.

In Fig. 8 it is observed that the energy consumption of the pass NF-1 with recycling is of 12.7 kWh/m^3 (with 0.96 m^3/h of permeate), compared to 9.24 kWh/m^3 that was previously obtained at the end of the pass NF-1 without recycle (also with one month of operation). The difference is explained by the increase in the content of solid material in the feed to the plant, which increases the fouling in the membrane affecting finally the flow of permeate. Although these energy levels coincide with previously reported data for plants of this size (<250 m^3/d) [14,15], they are higher than those achieved by large-size RO desalination plants (>10,000 m^3/d) [30]. It is important to note that the SEC indicated here corresponds to all the energy involved from the extraction of water at the source to the final product, and is also high by the low recovery when compared to a conventional system where recovery can reach 50%.

With regard to the operation of the second pass NF-2, the productivity remained constant in time because the feeding presented a low iron content and the turbidity of the watermarked practically 0.0 NTU.

The global recovery increased from 20.5% (Fig. 9) without recycling stream of rejection to 22.5% with recycling. The explanation for this increase is related to the mixture of the permeated product that was mostly done with what was obtained in the second pass NF-2, which did not present variations. It was obtained 0.87 m^3/h (14.5 L/min) in the pass NF-2 and was mixed with flows between 0.36 and 0.24 m^3/h (6 and 4 L/min) of the first pass NF-1, obtaining in this way the greater quantity of water produced.

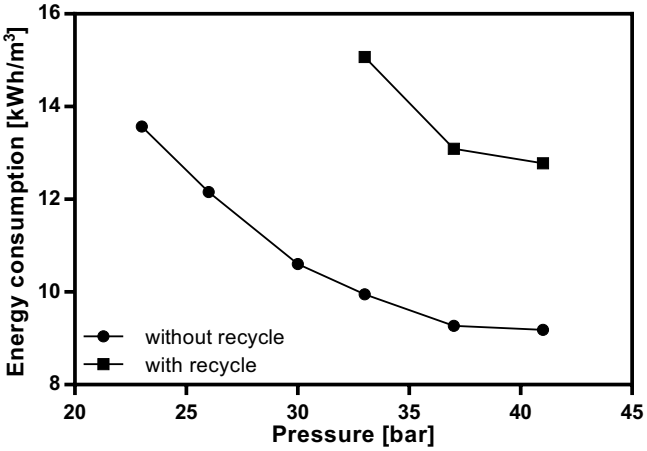

Fig. 8. Comparison of the energy consumption ratio by m^3 of water permeated in pass NF-1, when operating the plant with and without recycling of rejection.

If the two alternatives of operation of the plant are compared, it is concluded that the alternative with which it was obtained higher production times corresponds to that which includes recycling of the current of rejection (Fig. 10). However, this led to higher energy consumption than by operating the plant without recycling and forced membrane work since it was prematurely capped (by concentrating more salt in the inlet water), but it is justified by the fact to get a more permeated product in the day. The following figure is presented to have a quick comparison between the two alternatives.

It is observed that when operating the plant with recycling there was an increase in the ratio consumed energy/cubic meter of water produced because with that alternative, there was a greater duration of operation of the first pass NF-1, but this change increased the time of production and therefore a greater flow of permeate product. In addition, the overall recovery rate increased by 1.5%.

Fig. 11 shows that the rejection of salts did not present the same percentage value, being more favorable in the operation with seawater. This is only explained by the fact that

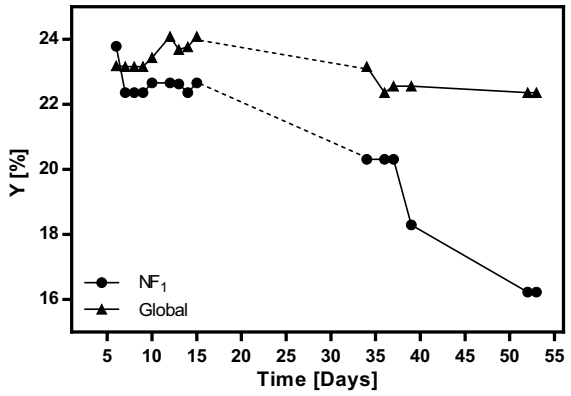

Fig. 9. Water recovery in first-pass NF-1 and global by two-pass of NF, with plant operation with recycle.

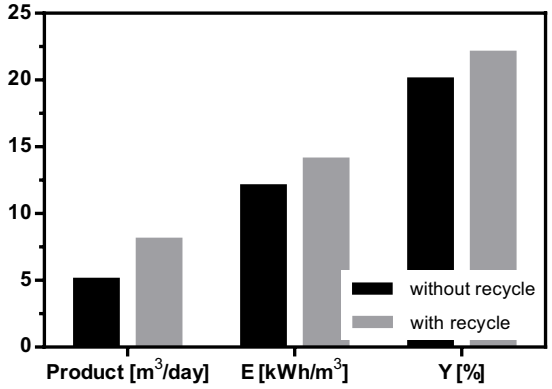

Fig. 10. Comparison of the most relevant characteristics between the two operating alternatives evaluated with brackish water.

Table 4
Chemical analysis of the drinking water obtained

Parameters	Unit	Result	NCh.409
Microbiological and turbidity parameters			
Total coliform	NMP/100 mL	<1.1	<5.0
Escherichia coli	NMP/100 mL	<1.1	<5.0
Turbidity	UNT	1.2	<2.0
Essential elements			
Copper	mg/L	<0.01	2.0
Total chromium	mg/L	<0.05	0.05
Fluoride	mg/L	<0.01	1.5
Iron	mg/L	<0.05	0.3
Manganese	mg/L	<0.05	0.1
Magnesium	mg/L	1.40	125.0
Selenium	mg/L	<0.005	0.01
Zinc	mg/L	<0.05	3.0
Non-essential elements or substances			
Arsenic	mg/L	<0.01	0.01
Cadmium	mg/L	<0.01	0.01
Cyanide	mg/L	<0.01	0.05
Mercury	mg/L	<0.001	0.001
Nitrate	mg/L	<0.01	50
Nitrite	mg/L	<0.005	3
Nitrato + nitrito ratio	–	<0.002	1
Lead	mg/L	<0.02	0.05
Parameters related to organoleptic characteristics			
True color	Unit Pt-Co	4	20
Smell	–	Odorless	Odorless
Flavor	–	Insipidus	Insipidus
Inorganic			
Ammonia	mg/L	<0.01	1.5
Chloride	mg/L	350	400
pH	Unit of pH	6.50	6.5 < pH < 8.5
Sulfate	mg/L	<0.01	500
Total dissolved solids	mg/L	590	1,500
Organic			
Phenolic compounds	μg/L	<1	2
Disinfection parameters			
Free chlorine	mg/L	<0.02	0.2 < C.L. < 2.0

Table 5
Costs associated (US$) with production in the desalination plant

Type of system	Nanofiltration plant	Average in reverse osmosis plants
Water production input		
Daily water production (m^3)	25	50
Variable costs		
Energy cost (%)	53.8	57.0
Chemicals (%)	7.7	9.6
Subtotal (%)	61.5	66.6
Fixed cost		
Membrane replacement (%)	18.2	9.5
Maintenance and labor (%)	20.3	23.9
Subtotal (%)	38.5	33.4
Cost of water production (US$/$m^3$)	0.70	1.9 [31]

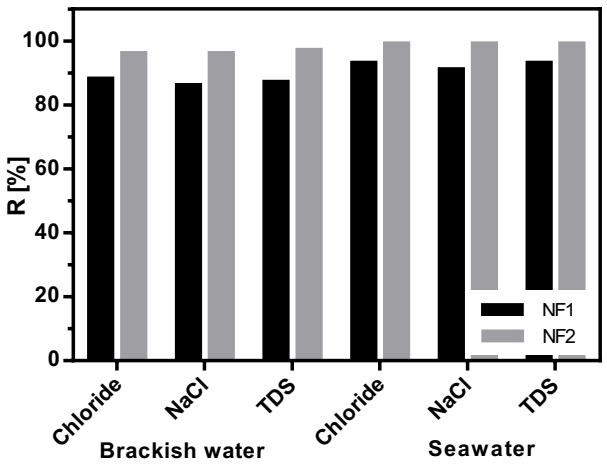

Fig. 11. Comparison of the percentages of rejection of salt, ion chloride and total solids dissolved between brackish water and seawater.

the brackish water used showed too much colloidal matter at the time of being treated with the NF membranes, which was deposited on the surface of these adding to the polarization by concentration and blocking of pores, reducing their performance.

The rejection of TDS of the first pass NF-1 reached 87.8% for brackish water compared with 93.65% of the rejection with seawater, while the global rejection reached values over 95%, a very acceptable value for classifying water as drinking water to despite the lower performance of the membrane. Table 4 shows that drinking water obtained meets all the requirements of the drinking water Chilean standard (NCh.409).

Finally, the general economic assessment of the plant process, which produces 25 m^3/d of drinking water, indicates that the drinking water is produced at a cost of US$ 0.70/m^3 (the cost of water production were calculated for our Plant OPEX). (Table 5). As other RO plants produce drinking water at a cost of US$ 1.9/m^3, the process using two-stage nanofiltration is very competitive [15,31]. Furthermore, the RO process generates highly pure water as a product, which requires to be remineralized. However, nanofiltration also allows the formulation of water for special purposes other than drinking, for example, water from the first nanofiltration pass can be used for personal cleanliness, toilet flushing, laundry or irrigation. In addition, nanofiltration allows for the production of water with different specifications since it works in two passes with variable operating conditions.

4. Conclusions

The proposed two-pass nanofiltration desalination system is capable of producing water for human consumption using seawater or brackish water at a cost of US$0.70/$m^3$, without major environmental impacts due to the low salinity of the reject water produced.

In the case of seawater desalination, a total recovery of 24% is achieved using a pressure of 40 bar in the first pass and 15 bar in the second. In the case of brackish water, under the same pressure conditions in the two passes, total recovery was achieved 22% and SEC 2 kWh/m^3 greater.

Acknowledgment

Author C.V. received funding from the CONICYT-PCHA/National Doctorate 2018 – 21181057.

References

[1] X.T. Zhao, R.N. Zhang, Y. Liu, M.G. He, Y.L. Su, C.J. Gao, Z.G. Jiang, Antifouling membrane surface construction: chemistry plays a critical role, J. Membr. Sci., 551 (2018) 145–171.
[2] D. Aitken, D. Rivera, A. Godoy-Faundez, E. Holzapfel, Water scarcity and the impact of the mining and agricultural sectors in Chile, Sustainability, 8 (2016) 128.
[3] S. Herrera-León, C. Cruz, A. Kraslawski, L.A. Cisternas, Current situation and major challenges of desalination in Chile, Desal. Water Treat., 171 (2019) 93–104.
[4] H. March, The politics, geography, and economics of desalination: a critical review, Wires Water, 2 (2015) 231–243.

[5] P.S. Goh, W.J. Lau, M.H.D. Othman, A.F. Ismail, Membrane fouling in desalination and its mitigation strategies, Desalination, 425 (2018) 130–155.
[6] N.R. Council, Desalination: A National Perspective, The National Academies Press, Washington, DC, 2008.
[7] M. Qasim, M. Badrelzaman, N.N. Darwish, N.A. Darwish, N. Hilal, Reverse osmosis desalination: a state-of-the-art review, Desalination, 459 (2019) 59–104.
[8] M.H. Liu, S.C. Yu, J. Tao, C.J. Gao, Preparation, structure characteristics and separation properties of thin-film composite polyamide-urethane seawater reverse osmosis membrane, J. Membr. Sci., 325 (2008) 947–956.
[9] A.L. Ahmad, B.S. Ooi, A. Wahab Mohammad, J.P. Choudhury, Development of a highly hydrophilic nanofiltration membrane for desalination and water treatment, Desalination, 168 (2004) 215–221.
[10] A.W. Mohammad, Y.H. Teow, W.L. Ang, Y.T. Chung, D.L. Oatley-Radcliffe, N. Hilal, Nanofiltration membranes review: recent advances and future prospects, Desalination, 356 (2015) 226–254.
[11] D. Zhou, L.J. Zhu, Y. Fu, M.G. Zhu, L.L. Xue, Development of lower cost seawater desalination processes using nanofiltration technologies—a review, Desalination, 376 (2015) 109–116.
[12] X.F. Lu, X.K. Bian, L.Q. Shi, Preparation and characterization of NF composite membrane, J. Membr. Sci., 210 (2002) 3–11.
[13] D.L. Oatley-Radcliffe, S.R. Williams, M.S. Barrow, P.M. Williams, Critical appraisal of current nanofiltration modelling strategies for seawater desalination and further insights on dielectric exclusion, Desalination, 343 (2014) 154–161.
[14] Y.L.G. de Schwarz, D. Cornwell, AWWA Research Foundation, Long Beach Water Department, A Novel Approach to Seawater Desalination Using Dual-staged Nanofiltration, American Water Works Association, Denver, United States, 2006.
[15] M.K. Wafi, N. Hussain, O. El-Sharief Abdalla, M.D. Al-Far, N.A. Al-Hajaj, K.F. Alzonnikah, Nanofiltration as a cost-saving desalination process, SN Appl. Sci., 1 (2019) 751.
[16] M.H. Liu, C.M. Zhou, B.Y. Dong, Z.F. Wu, L.Z. Wang, S.C. Yu, C.J. Gao, Enhancing the permselectivity of thin-film composite poly(vinyl alcohol) (PVA) nanofiltration membrane by incorporating poly(sodium-*p*-styrene-sulfonate) (PSSNa), J. Membr. Sci., 463 (2014) 173–182.
[17] M. Ernst, A. Bismarck, J. Springer, M. Jekel, Zeta-potential and rejection rates of a polyethersulfone nanofiltration membrane in single salt solutions, J. Membr. Sci., 165 (2000) 251–259.
[18] A.E. Childress, M. Elimelech, Effect of solution chemistry on the surface charge of polymeric reverse osmosis and nanofiltration membranes, J. Membr. Sci., 119 (1996) 253–268.
[19] M.D. Afonso, R.B. Yan˜ez, Nanofiltration of wastewater from the fishmeal industry, Desalination, 139 (2001) 429.
[20] D. Vial, G. Doussau, The use of microfiltration membranes for seawater pre-treatment prior to reverse osmosis membranes, Desalination, 153 (2003) 141–147.
[21] L. Bridgewater, E.W. Rice, APHA, AWWA, WEF, Standard Methods for the Examination of Water and Wastewater, 22nd ed., American Public Health Association, American Water Wealth Association, Water Environment Federation, Washington, D.C., USA, 2012.
[22] L.G. Peeva, E. Gibbins, S.S. Luthra, L.S. White, R.P. Stateva, A.G. Livingston, Effect of concentration polarisation and osmotic pressure on flux in organic solvent nanofiltration, J. Membr. Sci., 236 (2004) 121–136.
[23] N. Hilal, H. Al-Zoubi, A.W. Mohammad, N.A. Darwish, Nanofiltration of highly concentrated salt solutions up to seawater salinity, Desalination, 184 (2005) 315–326.
[24] S. Bunani, E. Yörükoğlu, G. Sert, Ü. Yüksel, M. Yüksel, N. Kabay, Application of nanofiltration for reuse of municipal wastewater and quality analysis of product water, Desalination, 315 (2013) 33–36.
[25] M. Mänttäri, A. Pihlajamäki, M. Nyström, Comparison of nanofiltration and tight ultrafiltration membranes in the filtration of paper mill process water, Desalination, 149 (2002) 131–136.
[26] K.L. Tu, L.D. Nghiem, A.R. Chivas, Boron removal by reverse osmosis membranes in seawater desalination applications, Sep. Purif. Technol., 75 (2010) 87–101.
[27] J. Wang, Y.M. Wang, J.Y. Zhu, Y. Zhang, J.D. Liu, B. Van der Bruggen, Construction of TiO_2@graphene oxide incorporated antifouling nanofiltration membrane with elevated filtration performance, J. Membr. Sci., 533 (2017) 279–288.
[28] S. Cortes, E. Reynaga-Delgado, A.M. Sancha, C. Ferreccio, Boron exposure assessment using drinking water and urine in the North of Chile, Sci. Total Environ., 410–411 (2011) 96–101.
[29] C.Y. Tang, T.H. Chong, A.G. Fane, Colloidal interactions and fouling of NF and RO membranes: a review, Adv. Colloid Interface Sci., 164 (2011) 126–143.
[30] J.B. Kim, K. Park, D.R. Yang, S.K. Hong, A comprehensive review of energy consumption of seawater reverse osmosis desalination plants, Appl. Energy, 254 (2019) 113652.
[31] M. Sarai Atab, A.J. Smallbone, A.P. Roskilly, An operational and economic study of a reverse osmosis desalination system for potable water and land irrigation, Desalination, 397 (2016) 174–184.